

## **Preparation, Characterization, and Quantum Chemical Investigation of New Schiff Base Complexes with Transition Metal Ions**

*Ansam A. Awad, Hider A. Mahdi*

*Department of Chemistry, College of Science, University of Thi-Qar, Nasiriyah, Thi-Qar 64001, Iraq*

**Abstract.** *Thiosemicarbazide and aromatic aldehyde are used to create the Schiff bases (L1, L2). Cu (II), Co, and Ni ions were added to these ligands to further complex them. Measurements of conductance, magnetic susceptibility, and Fourier transform infrared (FTIR) and H1NMR spectra have all been used to characterize the compounds. The ligands' spectrum data and density function theory were found to be in good agreement with their structures, demonstrating the great purity of every molecule.*

*The program of Hyperchem 8 have been used for theoretical accounts using PM3 method to study the electrostatic potential that provided good information about the complexity site. Of the result obtained we can suggest square planer geometry for Cu (II) complexes. The antioxidant activity of the syntheses compounds was evaluated by DPPH scavenger and these were showed a good antioxidant activity.*

**Keywords:** *Schiff base, ligand, complex, characterization, Dencity function theory.*

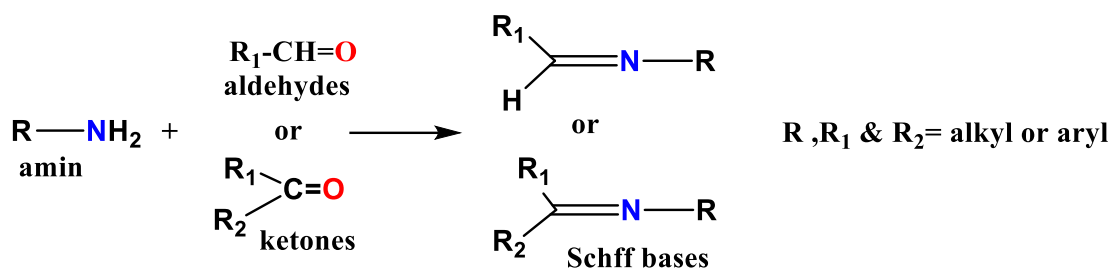
### **1. Introduction:**

The scientist Hugo Schiff (1864-1915) was from Germany. Schiff bases are the names he gave to the bases he found [1]. These chemicals have been around for 159 years, and because of their numerous applications in various disciplines, they continue to hold great significance for researchers and scientists [2,3]. A primary amine reacts with the carbonyl group of an aldehyde ( $RHC=O$ ) or ketone ( $R_2C=O$ ) [4,5] to create schiff base compounds (scheme.1). The nucleophilic addition reaction through the carbonyl group ( $C=O$ ) is the mechanism of the Schiff base.

The nucleophile is the primary amine which is reacts with the aliphatic or aromatic aldehyde or ketone to give an intermediate compound called carbinol amine. This intermediate compound was losing water molecule by hydrolyses process with acidic or basic media as a catalyst [5]. Imine or azomethine ( $-C=N-$ ) groups serve as the general function [6–10]. Because of their versatility, schiff bases are significant chemical substances in a variety of domains, including inorganic, analytical, and medicinal chemistry. When coordinated with various transition-metal ions, they can create a wide variety of stable complexes [11]. The Schiff base molecules' broad range of biological uses, including analgesic [12], anticancer [13–17], antimicrobial [16–17], antitumor [18,19], antioxidant [20–22], antiviral [23,24], and anti-inflammatory properties [25,26], depend on the presence of the imine linkage ( $-C=N-$ ). Additionally, Schiff bases are used as chemosensors [27], corrosion inhibitors [28,29], and dyes [30,31] in analytical chemistry, among other domains. Schiff bases typically consist of bi, tri, or tetra-dentate chelate ligands, as well as from extremely stable metal ion complexes [32]. When exposed to high temperatures and moisture, a number of Schiff base complexes exhibit exceptional catalytic activity in a variety of reactions [33]. Researchers have continued to be interested in the chemistry of metal complexes with Schiff base ligands that have nitrogen and oxygen as donor atoms [34]. Because of their biological characteristics, the transition metal complexes of Schiff base ligands containing O and N donor atoms are highly significant [35].

Because of their crucial roles in coordination chemistry, which stem from their straightforward preparation process and structural variation [39], Schiff bases and their copper (II) complexes have been the subject of much research [36–38].

It is confirmed that the coordination of copper (II) ion with bioactive ligands can actually improve their biological activity, for example Cu(II) complexes with hesperetin, naringenin and apigenin have shown higher inhibitory rate than their free ligands against human SGC-7901 (gastric cancer) and HepG2 (hepatocellular carcinoma) cell lines [40].



scheme.1 general synthesis of Schiff bases

## 2. Experiments

Every chemical and reagent utilized in this investigation was analytical grade and was acquired from Sigma-Aldrich. Thiosemicarbazide 98%, NiCl<sub>2</sub>·6H<sub>2</sub>O, CoCl<sub>2</sub>·6H<sub>2</sub>O, Cu acetate, 3-Ethoxy Salicylaldehyde, and 4-Methoxy Salicylaldehyde Using KBr pellets, the melting points of the produced compounds were determined using the SMP31 melting point apparatus and the Shimadzu FT-IR affinity spectrophotometer. The internal standard is TMS, even though their <sup>1</sup>H and <sup>13</sup>C NMR spectra were recorded in DMSO-d<sub>6</sub> using the Bruker 500MHz equipment. Using GERMANY-BG, electronic spectrum information was obtained (T60UV). A Perkin Elmer automated equipment was used for elemental micro analysis and work mass selective detector 5973.

### 2.1. There were two general procedures used to prepare Schiff base:

Method 1: A conical flask containing a mixture of aryl aldehyde (0.01 mol), thiosemicarbazide (0.01 mol, 1 g), and 5 ml of ethanol was placed in a microwave oven and exposed to 400 watts of radiation for five minutes. The title chemical was obtained as a lamellar crystal by recrystallizing the solid from the ethanol after it had cooled [41].

Method 2: A solution of aryl aldehyde (0.01 mol) in ethanol (10 mL) and a solution of thiosemicarbazide (0.01 mol, 1 g) in ethanol (10 mL) were combined, and a few drops of acetic acid were added as a catalyst. After four hours of heating the mixture to a reflux temperature, TLC was used to monitor the reaction. The title chemical was then obtained as a crystal by filtering the precipitation and recrystallizing the residue from the ethanol [42]. According to scheme (2)

### 2.2. Synthesis of metal complexes: The following method was utilized to create the Co, Ni, Cu complex of the obtained Schiff base:

dissolving (0.002 mol) of ligand in 10 mL of MeOH and a drop of DMF. Then, (0.2 g, 0.001 mol) of copper salt were added onto ligand's solution in round flask of 50 mL volume. Thereafter, the mixture was refluxed, heated, and continuously stirred for 4 hours. After completely reflux, mixture was left to perform cooling at room temperature for one hour. After solvent evaporation, the precipitation was filtered and recrystallized by the ethanol [42].

## 3. Results and Discussion

Two techniques were used to create the ligands (Schiff base). Way 1 has the advantage of taking the least amount of time to complete the synthesis of Schiff base when compared to Ways 1 and 2. In addition to having the highest yield, microwave irradiation synthesis has a quicker reaction time. The comparison of the two methods of Schiff base synthesis is displayed in Table 1.

Ligand	microwave irradiation	reflux
--------	-----------------------	--------

	time	yield	time	yield
L1	4 min	92	2.5 h	77
L2	7 min	85	3 h	73

3.1. The table (2) collected all of the ligand and its complexes' physicochemical characteristics and magnetic momentum information.

**Table 2: Molar conductance, magnetic susceptibility, and physical characteristics**

compound	Colour	M.P	$\Lambda_m$ s.cm <sup>2</sup> . mol <sup>-1</sup>	$\mu_{eff}$ B.M
C <sub>9</sub> H <sub>11</sub> N <sub>3</sub> O <sub>2</sub> S (L <sub>1</sub> )	White	160-163	----	
C <sub>18</sub> H <sub>21</sub> C <sub>12</sub> N <sub>5</sub> NiO <sub>4</sub> S <sub>2</sub>	Brown	220-222	7.68	2.83
C <sub>9</sub> H <sub>15</sub> C <sub>12</sub> CoN <sub>3</sub> O <sub>4</sub> S	Black	248-250	20.30	3.87
C <sub>22</sub> H <sub>28</sub> CuN <sub>6</sub> O <sub>8</sub> S <sub>2</sub>	Light brown	222-224	3.21	1.73
C <sub>10</sub> H <sub>13</sub> N <sub>3</sub> O <sub>2</sub> S (L <sub>2</sub> )	White	235-237	-----	
C <sub>20</sub> H <sub>28</sub> C <sub>12</sub> N <sub>6</sub> NiO <sub>6</sub> S <sub>2</sub>	Mint green	222-228	45.2	0
C <sub>14</sub> H <sub>19</sub> CoN <sub>3</sub> O <sub>6</sub> S	Deep brown	249	3.78	3.8
C <sub>14</sub> H <sub>18</sub> CuN <sub>3</sub> O <sub>6</sub> S	Black	195	3.16	1.73

### 3.2 FT-IR spectral

Using KBr disc for to ligands and their complexes, FT-IR of the synthetic ligand and its complexes was performed; all FTIR data were collected and recorded in table (3). The azomethine bands of the complex were visible at (1580)-(1600) cm<sup>-1</sup>, whereas the azomethine bands of the free ligand (L) were visible at (1600)-(1631) cm<sup>-1</sup>. There were new bands founded. ascribed to the (N-H) and (C-O) bonds, which were found at the 1026–1396 cm<sup>-1</sup> and 3398–3495 cm<sup>-1</sup> regions, respectively. According to table (3) and the pictures, this suggests that the coordinate was formed by the (N) and (O) atoms. (6-8).



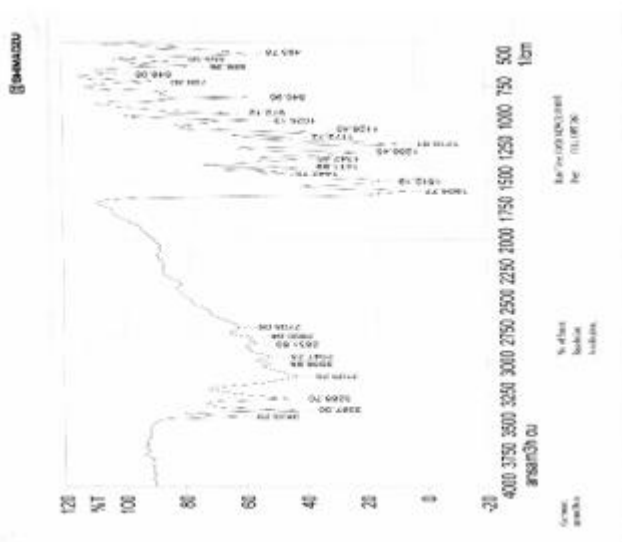


**Table (3) Infrared spectra of Ligand and its metal complexes ( $\nu$   $\text{cm}^{-1}$ )**

No.	$\nu$ (O-H)	$\nu$ (C-H) aromatic	$\nu$ (C-H) aliphatic	$\nu$ (C=N) azomethane	$\nu$ (C=C)	$\nu$ (C-O)	C=S	N-H
L <sub>1</sub>	3360	3155	2981	1631	1597.0	1099.4	848	3471
L <sub>1</sub> Co	3317.5	3178.6	2939.5	1604.7	1519.9	1026.4	833	3490
L <sub>1</sub> Ni	3302	3194.1	2962.6	1604.77	1543.0	1026.13	840.9	3425
L <sub>1</sub> Cu	3387	3286.7	2947.2	1604.7	1512.1	1026.13	840	3433
L <sub>2</sub>	3302	3251.9	2970	1600.9	1581.6	1396.4	829	3398.5
L <sub>2</sub> Co	3302	3194	2978	1604.7	1512	1311	894	3441
L <sub>2</sub> Ni	3317	3194	2978	1612	1543	1350	825.5	3450
L <sub>2</sub> Cu	3317	3155	2979	1604	1550	1303	848.6	3495

### 3.3. Nuclear Magnetic Resonance

<sup>1</sup>H-NMR (DMSO-d<sub>6</sub>,  $\delta$  in ppm) L<sub>1</sub>: 11.28 (s, 1H, OH), 8.04 (s, 1H, CH=N1), 6.41-6.45 (d, 2H, H<sub>4</sub>, Ar-H<sub>1</sub>), 7.80-7.85 (m, 1H, Ar-H), 9.96, (s, 1H, NH), 8.28 (s, 1H, NH), 3.73 (s, 3H, OCH<sub>3</sub>), 3.73, (cis/trans ratio: 3/2, s, 3H, N4-CH<sub>3</sub>).

<sup>1</sup>H-NMR (DMSO-d<sub>6</sub>,  $\delta$  in ppm): 11.42 (s, 1H, OH), 8.14 (s, 1H, CH=N1), 6.73-8.14 (m, 3H, Ar-H), 9.02, (s, 1H, NH), 8.42 (s, 1H, NH), 1.32-1.36 (t, 3H, CH<sub>3</sub>), 4.01-4.07 (q, 2H, O-CH<sub>2</sub>).

The thione carbon (C=S) was identified by a downfield resonance at  $\delta$  177.6 ppm in compound L<sub>1</sub>'s <sup>13</sup>C NMR study. The heteroaromatic system's C-O and C=N carbons were responsible for additional signals at  $\delta$  162.3–158.3 ppm, whilst aromatic CH and quaternary carbons were detected between  $\delta$  140.7 and 101.2 ppm. The presence of the methoxy substituent was confirmed by a clear resonance at  $\delta$  55.6 ppm. These findings confirm the methoxy-substituted thiosemicarbazone derivative's structural integrity.

Compound L<sub>2</sub>'s <sup>13</sup>C NMR spectrum showed the thione carbon (C=S) at  $\delta$  178.1 ppm in addition to heteroaromatic carbon resonances at  $\delta$  147.4–140.2 ppm and  $\delta$  121.2–114.5 ppm. The two distinctive peaks of the alkoxy group were  $\delta$  64.6 ppm (O-CH<sub>2</sub>) and  $\delta$  15.1 ppm (terminal CH<sub>3</sub>). These characteristics support the suggested thiosemicarbazone structure by confirming that an ethoxy substituent has replaced the methoxy group.

### 3.4. Mass spectra

The mass spectra of Co,Cu,Ni complexes appeared molecular ion peak at 391.12 m/z for [CoL<sub>1</sub>(H<sub>2</sub>O)<sub>2</sub>.Cl<sub>2</sub>], 632.16 m/z for [Cu(L<sub>1</sub>)<sub>2</sub>(CH<sub>3</sub>COO)<sub>2</sub>], 565.10 m/z for [Ni(L<sub>1</sub>)<sub>2</sub>Cl<sub>2</sub>], 642.19m/z, [Ni(L<sub>2</sub>)<sub>2</sub>]Cl<sub>2</sub>.2H<sub>2</sub>O, m/z for 391.86 [CuL<sub>2</sub>(HCOO)<sub>2</sub>] and m/z for 416.31 [CoL<sub>2</sub>(CH<sub>3</sub>COO)<sub>2</sub>] which is in conformity with the molecular formula C<sub>9</sub>H<sub>15</sub>Cl<sub>2</sub>CoN<sub>3</sub>O<sub>4</sub>S, C<sub>22</sub>H<sub>28</sub>CuN<sub>6</sub>O<sub>8</sub>S<sub>2</sub>, C<sub>18</sub>H<sub>21</sub>Cl<sub>2</sub>N<sub>5</sub>NiO<sub>4</sub>S<sub>2</sub>, C<sub>12</sub>H<sub>14</sub>CuN<sub>3</sub>O<sub>6</sub>S and C<sub>14</sub>H<sub>19</sub>CoN<sub>3</sub>O<sub>6</sub>S

respectively. As shown in fig. (12-14).[43]

### 3.5. Conductivity Measurements.

At room temperature, the synthetic compounds' molar conductance values in 104M ethanol were measured. The produced molecules were nonelectrolyte, as evidenced by conductance values below (3.16-45.2)  $\text{s}\cdot\text{cm}^2\cdot\text{mol}^{-1}$  [15, 16]. This implied that anions were not present outside the complexes' coordination area.

### 4. TGA/DSC

The free ligand's thermogram shows several stages of degradation: First stage: ascribed to the elimination of physically adsorbed and/or lattice water molecules (29–147 °C, peak at 122 °C,  $\Delta H = 161.8 \text{ J/g}$ ).

The second stage (222–242 °C, peak at 229 °C,  $\Delta H = 70.6 \text{ J/g}$ ): represents the imine ( $-\text{C}=\text{N}-$ ) linkage's partial breakdown.

The breakdown of the organic backbone is linked to major decomposition (237–350 °C, weight loss  $\approx 80.4\%$ ,  $\Delta H = 345.7 \text{ J/g}$ ), which suggests moderate thermal stability.

The breakdown of any remaining carbonaceous fragments is represented by the last stage, which occurs between 382 and 424 °C. These processes were validated by the DSC curve, which showed clear endothermic peaks and indicated that the free Schiff base is fully broken down before 450 °C. The Schiff Base Complex of Ni(II).

The Ni(II) complex showed improved stability and a notably altered thermal profile: First stage: partial imine moiety breakdown and loss of coordinated water molecules (220–303 °C, peak at 262 °C).

The second stage involves the breakdown of the organic ligand framework while preserving the metal–ligand coordination environment (336–392 °C, peak at 363 °C,  $\Delta H = 208 \text{ J/g}$ , weight loss  $\approx 70\%$ ).

Third stage: breakage of aromatic fragments (325–418 °C, peak at 361 °C).

The complex completely decomposes in the last stage (461–492 °C, strong peak at 476 °C,  $\Delta H = 1379 \text{ J/g}$ ), forming a stable inorganic residue that is recognized as NiO with a residual mass of about 897 mg.

The free Schiff base ligand underwent a thorough breakdown in several phases, according to the thermal analysis (TGA/DSC) L2 and L2Cu. The elimination of physically adsorbed or lattice water was thought to be the cause of the initial weight loss below 250 °C. The breakdown of the organic backbone, primarily the  $-\text{CH}=\text{N}-$  and aromatic moieties, was attributed to a significant degradation step that took place between 226 and 370 °C with a mass loss of around 57%. The ligand was nearly completely lost during further breakdown up to 620 °C, leaving no stable residue behind, confirming the compound's organic nature.

The Cu(II)–Schiff base combination, on the other hand, showed greater thermal stability. Up to 270 °C, the initial weight loss ( $\sim 4\%$ ) was correlated with the release of weakly bound water and solvent molecules.

Subsequent degradation steps between 270–600 °C were related to the decomposition of the coordinated ligand framework. Unlike the free ligand, the complex left a stable residue ( $\sim 10\%$ ) at 900 °C, which is consistent with the formation of thermally stable copper oxide.

These findings indicate that coordination with copper enhances the thermal stability of the Schiff base ligand, alters its decomposition pathway, and results in a stable inorganic residue at elevated temperatures.[44]

## 5. DFT Computational Report

### 5.1. Introduction

Density Functional Theory (DFT) provides valuable insights into the electronic structure of molecules. The frontier molecular orbitals, namely the Highest Occupied Molecular Orbital (HOMO) and Lowest Unoccupied Molecular Orbital (LUMO), are critical in predicting the stability and reactivity of chemical species. Global reactivity descriptors such as ionization potential (IP), electron affinity (EA), hardness ( $\eta$ ), softness ( $\delta$ ), electronegativity ( $\chi$ ), and electrophilicity ( $\omega$ ) help in understanding the chemical behavior and possible biological applications.

## 5.2. Computational Methodology

The calculations were performed using Density Functional Theory (DFT) with the B3LYP functional and the 3-21G basis set. The HOMO and LUMO energy values were used to calculate the energy gap ( $\Delta E$ ), which is an indicator of molecular stability and reactivity. Other reactivity descriptors were obtained according to Koopman's theorem and Parr's definitions.

## 5.3. Results and Discussion

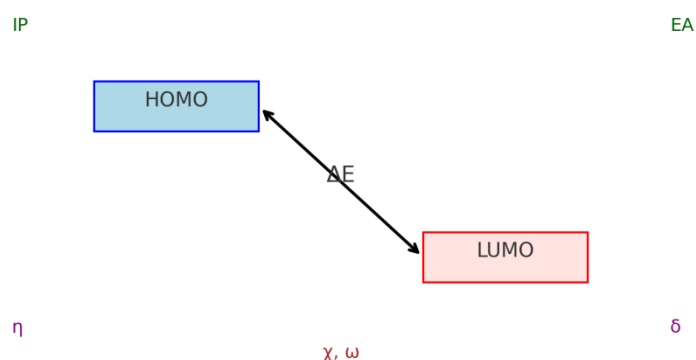
**Table 4. Calculated quantum chemical descriptors using B3LYP/3-21G.**

Compound	HOMO (eV)	LUMO (eV)	$\Delta E$ (eV)	IP (eV)	EA (eV)	Hardness $\eta$ (eV)	Softness $\delta$	Electronegativity $\chi$ (eV)	Electrophilicity $\omega$ (eV)
Compound 1	-0.20248	-0.09284	0.10964	0.20248	0.09284	0.05482	9.12076	-0.14766	0.19886
Compound 2	-0.17893	-0.08149	0.09744	0.17893	0.08149	0.04872	10.26272	-0.13021	0.174

## 5.4. Graphical Abstract

The schematic illustration below summarizes the relationship between HOMO, LUMO, the energy gap ( $\Delta E$ ), and the associated global reactivity descriptors (IP, EA,  $\eta$ ,  $\delta$ ,  $\chi$ ,  $\omega$ ).

Graphical Abstract: Frontier Orbitals & Descriptors



## 5.5. Extended Discussion

The analysis of the frontier molecular orbitals (HOMO and LUMO) provides critical insights into the electronic properties of the studied compounds. The HOMO represents the electron-donating ability, while the LUMO reflects the electron-accepting capacity. Compound 1 has a slightly lower HOMO energy (-0.202 eV) compared to Compound 2 (-0.179 eV), suggesting that Compound 2 is a stronger electron donor and therefore more susceptible to oxidation. Conversely, the LUMO of Compound 1 (-0.093 eV) is lower than that of Compound 2 (-0.081 eV), indicating that Compound 1 is the better electron acceptor and hence more prone to reduction.

The HOMO–LUMO energy gap ( $\Delta E$ ) is a key parameter for assessing molecular reactivity and stability. Compound 1 exhibits a gap of 0.110 eV, while Compound 2 has a smaller gap of 0.097 eV. The reduced gap in Compound 2 implies higher chemical reactivity and lower kinetic stability, which can enhance its potential biological activity by facilitating interactions with biomolecular targets. On the other hand, Compound 1, with a larger gap, is expected to be more chemically stable but less

reactive.

Ionization potential (IP) and electron affinity (EA) further support these observations. Compound 1 has an IP of 0.202 eV, slightly higher than Compound 2 (0.179 eV), implying that Compound 2 can lose electrons more easily. In terms of EA, Compound 1 (0.093 eV) shows a stronger electron-accepting ability compared to Compound 2 (0.081 eV). These findings are consistent with the HOMO/LUMO analysis.

Global reactivity descriptors refine this interpretation. Compound 1 exhibits greater hardness ( $\eta = 0.055$  eV) than Compound 2 ( $\eta = 0.049$  eV), meaning it is more resistant to charge transfer. The corresponding softness values show the opposite trend, with Compound 2 being softer ( $\delta = 10.26$ ) than Compound 1 ( $\delta = 9.12$ ), indicating higher reactivity. Electronegativity ( $\chi$ ) is slightly higher in Compound 1 (-0.148 eV) than in Compound 2 (-0.130 eV), highlighting its stronger electron-attracting nature. Electrophilicity ( $\omega$ ) also follows this pattern: Compound 1 has a higher value (0.199 eV) compared to Compound 2 (0.174 eV), confirming its stronger tendency to act as an electrophile.

Taken together, these descriptors present a complementary picture: Compound 1 is more electrophilic and chemically stable, while Compound 2 is more reactive and chemically flexible. This suggests that Compound 2 may have enhanced biological activity due to its higher reactivity and softer electronic character, while Compound 1 could provide stability and selectivity in potential applications.[45]

### 5.6. Additional Graphical Analysis

**Figure 2. Comparison of HOMO and LUMO energy levels for the studied compounds.**

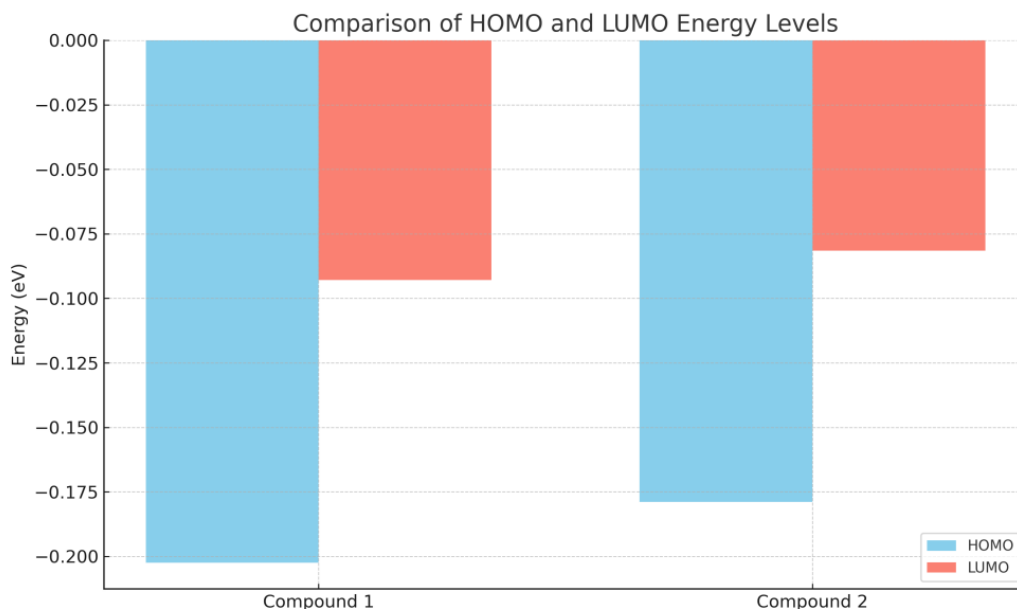


**Figure 3. Comparison of global reactivity descriptors ( $\eta$ ,  $\delta$ ,  $\chi$ ,  $\omega$ ) between the compounds.**

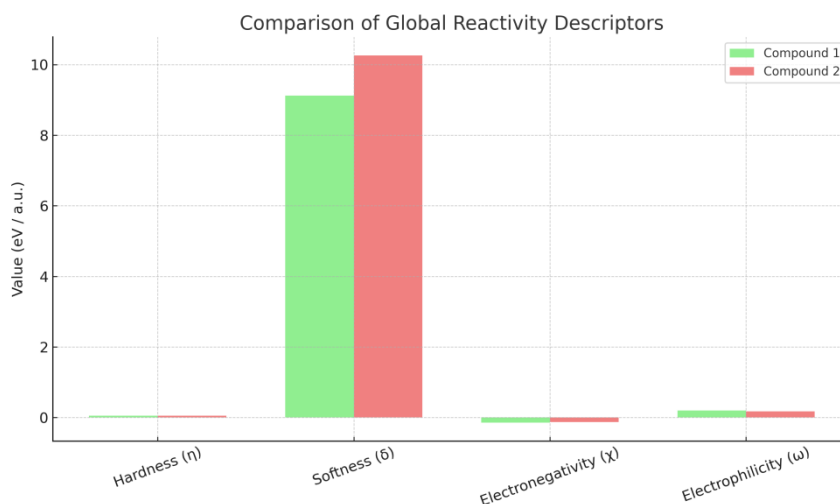
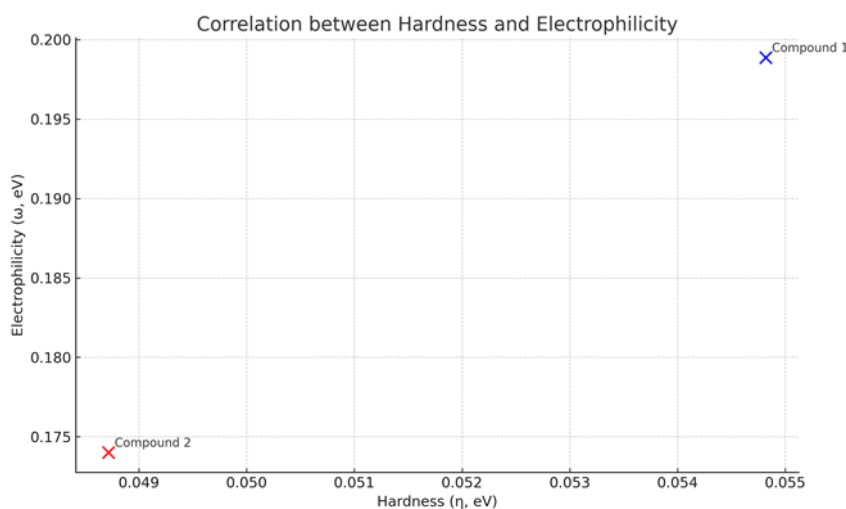


**Figure 4. Scatter plot illustrating the relationship between hardness ( $\eta$ ) and electrophilicity ( $\omega$ ).**



## REFERENCES

1. Qin, W., Long, S., Panunzio, M. and Biondi, S., "Schiff Bases: A short survey on an evergreen chemistry tool". *Molecules*, 18(10), 12264-12289, 2013.
2. Khachatryan G.E., Mkrtychyan N.I., Gavalyan V.B., "Antibacterial Pproperties of new Chitosan-based Schiff-base", *Int. J. Adv. Res.*, 2018, 6:1187
3. Ghosh, P., Dey, S.K., Ara, M.H., Karim, K.Md.R. and Islam, A.B.M.N., "A Review on synthesis and versatile applications of some selected Schiff bases with their transition metalcomplexes", *Egypt. J. Chem.*, 62 (2), 523-547, 2019.
4. Mukhtar, S.S., Hassan, A.S., Morsy, N.m., Hafez, T.S, Hassaneen, H.M., Saleh, F.M., "Overview on Synthesis, Reactions, Applications, and Biological Activities of Schiff Bases", *Egypt. J. Chem.*, 64(11), 6541 – 6554, 2021.
5. Ahmed, A.A., Al-mashhadani, M.H., Hashim, H., Ahmed, D.S., Yousif, E., "Morphological, Color Impact and Spectroscopic Studies of New Schiff Based DerivedFrom 1,2,4-Triazole Ring. Progress in Color", *Colorantsand Coatings*, 14, 27-34, 2021.
6. Ashraf, M.A., Mahmood, K., Wajid, A., "Synthesis, Characterization and Biological Activity of Schiff Bases", *IPCBE*, 10, 1–7, 2011,
7. Kathiresan, S., Annaraj, J., Bhuvanesh, N.S., "Cu (II) and Ni (II) Complexes of Anthracene-Affixed Schiff Base: A Conflict betweenCovalent and Stacking Interactions with DNA Bases", *Chemistry Select*, 2, 5475–5484, 2017.

8. Nowicka, A., Liszkiewicz, H., Paulina, W. "Schiff Bases-Selected Syntheses, Reactions and Biological Activity", *Wiadomo´sci Chem.*, 68, 3-4, 2014.
9. Da Silva, C.M., da Silva, D.L., Modolo, L.V., Alves, R.B., de Resende, M.A., Martins, C.V.B., de Fátima, Â. "Schiff Bases: A Short Review of Their Antimicrobial Activities", *J. Adv. Res.*, 2, 1-8, 2011.
10. Xavier, A., Srividhya, N., "Synthesis and Study of Schiff Base Ligands", *IOSR J. Appl. Chem.*, 7, 6-15, 2014.
11. Al-Hakimi, A.N., Alminderej, F., Aroua, L., Alhag, S.K., Alfaifi, M., Y., M, S.O., Mahyoub, J.A., Eldin I. Elbehairi, S., Alnafisah, A.S., "Design, synthesis, characterization of zirconium (IV), cad-mium (II) and iron (III) complexes derived from Schiff base 2-mium (II) and iron (III) complexes derived from Schiff base 2-aminomethylbenzimidazole, 2-hydroxynaphtadehyde and evalua-tion of their biological activity", *Arab. J. Chem.*, 13, 7378-7389, 2020.
12. Yassen, T.M., AL-Azzawi, A.M., "Synthesis and Characterization of New Bis-Schiff Bases Linked to Various Imide Cycles", *Iraqi Journal of Science*, 64(3), 1062-1070, 2023.
13. Alorini, T.A., Al-Hakimi, A.N., Saeed, S.E., Alhamzi, E.H.L. & Albadri, A.E.A.E., "Synthesis, characterization, and anticancer activity of some metal complexes with a new Schiff base ligand", *Arabian J Chem.*, 15(2), 103559, 2022.
14. Omer, A.M., Eltaweil, A.S., El-Fakharany, E.M., Abd El-Monaem, E.M., Magda M. F. Ismail M.M.F., Mohy-Eldin, M.S. & Ayoup, M.S., "Novel Cytocompatible Chitosan Schiff Base Derivative as a Potent Antibacterial, Antidiabetic, and Anticancer Agent", *Arabian Journal for Science and Engineeri*, 1-15, 2023.
15. Alasadi, Y.K., Jumaa, F.H., Mukhlif, M.G. & Shawkat, S.M., "Preparation, Characterization, Anti-cancer and Antibacterial Evaluation of New Schiff base and Tetrazole Derivatives", *Tikrit Journal of Pure Science*, 28 (2), 12-19, 2023.
16. Shayma L. Abdulhadi, Maadh Q. Abdulkadir, May M. Al-Mudhafar, "The Importance of 2-AminoThiazole Schiff Bases as Antimicrobial and Anticancer Agents," *Al-Mustansiriyah Journal of Science*, 31(3), 46-64, 2020.
17. Aroua, L.M, Alhag, S.K., Al-Shuraym, L.A, Messaoudi, S., Mahyoub J. A., Alfaifi, M.Y., Al-Otaibi, W.M., "Synthesis and characterization of different complexes derived from Schiff base and evaluation as a potential anticancer, antimicrobial, and insecticide agent", *Saudi J Biol Sci.*, 30(3), 103598, 2023.
18. Aguilar-Llanos, E., Carrera-Pacheco, S.E., González-Pastor, R., Zúñiga-Miranda, J., Cristina Rodríguez-Pólit, C., Carlos Romero-Benavides, J.C. & Heredia-Moya, J., "Synthesis and Evaluation of Biological Activities of Schiff Bas Derivatives of 4-Aminoantipyrene and Cinnamaldehyde", *Chem. Proc.* 4, 1-9, 2022.
19. Luis A. Alfonso-Herrera, Sharon Rosete-Luna, Delia Hernández-Romero, José M. Rivera-Villanueva, José L. Olivares-Romero, J. Antonio Cruz-Navarro, Anell Soto-Contreras, "Transition Metal Complexes with Tridentate Schiff Bases (ONO and ONN) Derived from Salicylaldehyde: An Analysis of Their Potential Anticancer Activity", *ChemMedChem.*, 17(20), 1-47, 2022
20. Awolope, O.R., Ejidike, I.P. & Clayton, H.S., "Schiff base metal complexes as a dual antioxidant and antimicrobial agents", *Journal of Applied Pharmaceutical Science*, 13(03), 132-140, 2023.
21. Rezaei, M.T., Keypour, H., Hajari, S., yaghoobi F., Farida S.H.M., Saadati, M. & Gable R.W., "Theoretical and solid-state structures of three new macrocyclic Schiff base complexes and the investigation of their anticancer, antioxidant and antibacterial properties", *RSC Adv.*, 13, 9418-9427, 2023.
22. Aytac, S., Gundogdu, O., Bingol, Z. & Gulcin, I., "Synthesis of Schiff Bases Containing Phenol Rings and Investigation of Their Antioxidant Capacity, Anticholinesterase,

- Butyrylcholinesterase, and Carbonic Anhydrase Inhibition Properties”, *Pharmaceutics*, 15(3), 779, 2023.
23. Abd El-Hamid, S.M., Sadeek, S.A., Mohammed, S.F., Ahmed, F.M., El-Gedamy, M.S, “N<sub>2</sub>O<sub>2</sub>-chelate metal complexes with Schiff base ligand: Synthesis, characterisation and contribution as a promising antiviral agent against human cytomegalovirus”, *Applied Organometallic Chemistry*, 37(2), 6925, 2023.
  24. Flifel, I. A. Synthesis, Characterization and Anticancer Study of New 3-[(2Z)-2 (2-hydroxybenzylidene) hydrazinyl]-5-(2-hydroxyphenyl)-1, 3, 4-oxadiazol-3-ium and its Transition Metal Complexes. *University of Thi-Qar Journal of Science*, 10(2), 98-102., 2023.
  25. Mihsen, H. H. Synthesis, Characterization, and Biological Activity of Copper (II) Complexes Containing Bidentate Schiff Bases. *University of Thi-Qar Journal of Science*, 4(2), 59-65. 2014.
  26. Krishna, G. A., Dhanya, T. M., Shanty, A. A., Raghu, K. G., & Mohanan, P. V.,” Transition metal complexes of imidazole derived Schiff bases: Antioxidant/anti-inflammatory/antimicrobial/enzyme inhibition and cytotoxicity properties”, *Journal of Molecular Structure*, 1274, 134384, 2023.
  27. Ejiah, F. N., Rofiu, M. O., Oloba-Whenu, O. A., & Fasina, T. M. “Schiff bases as analytical tools: synthesis, chemo-sensor, and computational studies of 2-aminophenol Schiff bases”, *RSC Adv.*, 13(5), 2756-2767, 2023.
  28. Boulechfar, C., Ferkous, H., Delimi, A., Berredjem, M., Kahlouche, A., Madaci, A. & Benguerba, Y., “Corrosion inhibition of Schiff base and their metal complexes with [Mn (II), Co (II) and Zn (II)]: Experimental and quantum chemical studies”, *Journal of Molecular Liquids*”, 378, 121637, 2023.
  29. Al-Amiery, A. A., Betti, N., Isahak, W. N. R. W., Al-Azzawi, W. K., & Wan Nik, W. M. N., “Exploring the Effectiveness of Isatin–Schiff Base as an Environmentally Friendly Corrosion Inhibitor for Mild Steel in Hydrochloric Acid. *Lubricants*”, 11(5), 211, 2023.
  30. Ayodhya, D., “Fabrication of SPR triggered Ag-CuO composite from Cu (II)-Schiff base complex for enhanced visible-light-driven degradation of single and binary-dyes and fluorometric detection of nitroaromatic compounds. *Inorganic Chemistry Communications*”, 148, 110295, 2023.
  31. Rajimon, K. J., Elangovan, N., Khairbek, A. A., & Thomas, R., “Schiff bases from chlorine substituted anilines and salicylaldehyde: Synthesis, characterization, fluorescence, thermal features, biological studies and electronic structure investigations”, *Journal of Molecular Liquids*, 370, 121055, 2023.
  32. Dr. A. Xavier<sup>1</sup>, N. Srividhya<sup>2</sup>, “Synthesis and Study of Schiff base Ligands”, *IOSR-JAC.*, 7(11), 6-15, 2014.
  33. Dalia, S. A., Afsan, F., Hossain, M. S., Khan, M. N., Zakaria, C., Zahan, M. K. E., & Ali, M., “A short review on chemistry of schiff base metal complexes and their catalytic application”, *Int. J. Chem. Stud.*, 6, 2859-2866, 2018.
  34. Ommenya, F. K., Nyawade, E. A., Andala, D. M., & Kinyua, J., “Synthesis, characterization and antibacterial activity of Schiff base, 4-Chloro-2-[(E)-[(4-fluorophenyl) imino] methyl} phenol metal (II) complexes”, *Journal of Chemistry*, 2020, 1-8, 2020.
  35. Sumrta, S. H., Ibrahim, M., Ambreen, S., Imran, M., Danish, M., & Rehmani, F. S., “Synthesis, spectral characterization, and biological evaluation of transition metal complexes of bidentate N, O donor Schiff bases”, *Bioinorganic chemistry and applications*, 2014, 1-10, 2014.
  36. López-Gastélum, K.A., Velázquez-Contreras, E.F., García, J.J., Flores-Alamo, M., Aguirre, G., Chávez-Velasco, D., Narayanan, J., Rocha-Alonzo, F. Mononuclear and tetranuclear copper(I) complexes bearing amino acid schiff base ligands: Structural characterization and catalytic applications”, *Molecules*, 26, 7301, 2021.

37. Pitucha, M., Korga-Plewko, A., Czyrkowska, A., Rogalewicz, B., Drozd, M., Iwan, M., Kubik, J., Humeniuk, E., Adamczuk, G., Karczmarzyk, Z., “Influence of complexation of thiosemicarbazone derivatives with Cu (II) ions on their antitumor activity against melanoma cells”, *Int. J. Mol. Sci.*, 22, 3104, 2021.
38. Al-Shboul, T.M.A.; El-khateeb, M.; Obeidat, Z.H.; Ababneh, T.S.; Al-Tarawneh, S.S.; Al Zoubi, M.S.; Alshaer, W.; Abu Seni, A.; Qasem, T.; Moriyama, H.; et al. “Synthesis, Characterization, Computational and Biological Activity of Some Schiff Bases and Their Fe, Cu and Zn Complexes”, *Inorganics*, 10, 112, 2022.
39. Yusuf, T.L., Oladipo, S.D., Zamisa, S., Kumalo, H.M., Lawal, I.A., Lawal, M.M., Mabuba, N. “Design of New Schiff-Base Copper(II) Complexes: Synthesis, Crystal Structures, DFT Study, and Binding Potency toward Cytochrome P450 3A4”, *ACS Omega*, 6, 13704–13718, 2021.
40. Wang, H.; Tan, M.; Zhu, J.; Pan, Y.; Chen, Z.; Liang, H.; Liu, H. “Synthesis, cytotoxic activity, and DNA binding properties of copper (II) complexes with hesperetin, naringenin, and apigenin”. *Bioinorg. Chem. Appl.*, 2009, 347872, 2009.
41. Yang, Z., & Sun, P., “Compare of three ways of synthesis of simple Schiff base”, *Molbank*, 2006(6), M514, 2006.
42. Kailas, K. H., Sheetal, J. P., Anita, P. P., & Apoorva, H. P., “Four synthesis methods of schiff base ligands and preparation of their metal complex with Ir and antimicrobial investigation”, *World Journal of Pharmacy and Pharmaceutical Sciences*, 5(2), 1055-1063, 2016.
43. Jayanthi, K., Meena, R. P., Chithra, K., Kannan, S., Shanthi, W., Saravanan, R., ... & Satheesh, D. Synthesis and microbial evaluation of copper (II) complexes of Schiff base ligand derived from 3-methoxysalicylaldehyde with semicarbazide and thiosemicarbazide. *Journal of Pharmaceutical, Chemical and Biological Sciences*, 5(3), pp. 205-215, 2017.
44. de Moura, A., Júnior, J. B., Carvalho, A. C. S., & Caires, F. J. Green synthesis of a Schiff base ligand and its Co (II), Cu (II) and Zn (II) complexes: thermoanalytical and spectroscopic studies. *Journal of Thermal Analysis and Calorimetry*, 147(20), 11093-11106, 2022.
45. Olalekan, T. E., Akintemi, E. O., Van Brecht, B., & Watkins, G. M. Synthesis, characterization and DFT studies of Schiff bases of p-methoxysalicylaldehyde. *Bulletin of the Chemical Society of Ethiopia*, 37(3), 675-688, 2023.

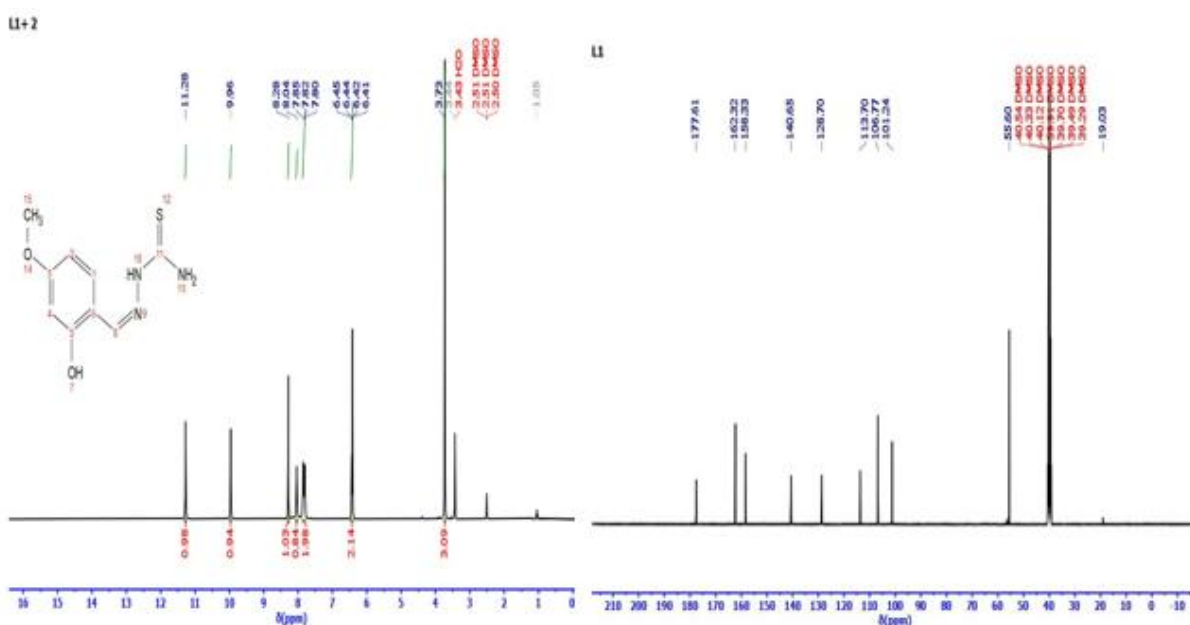
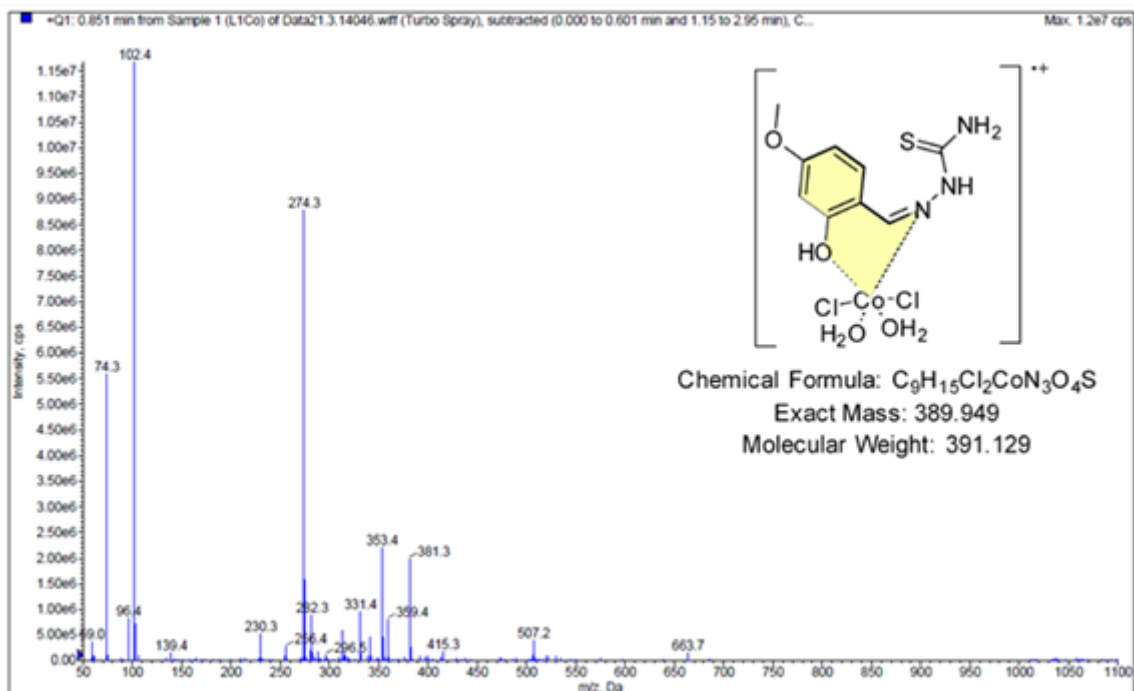
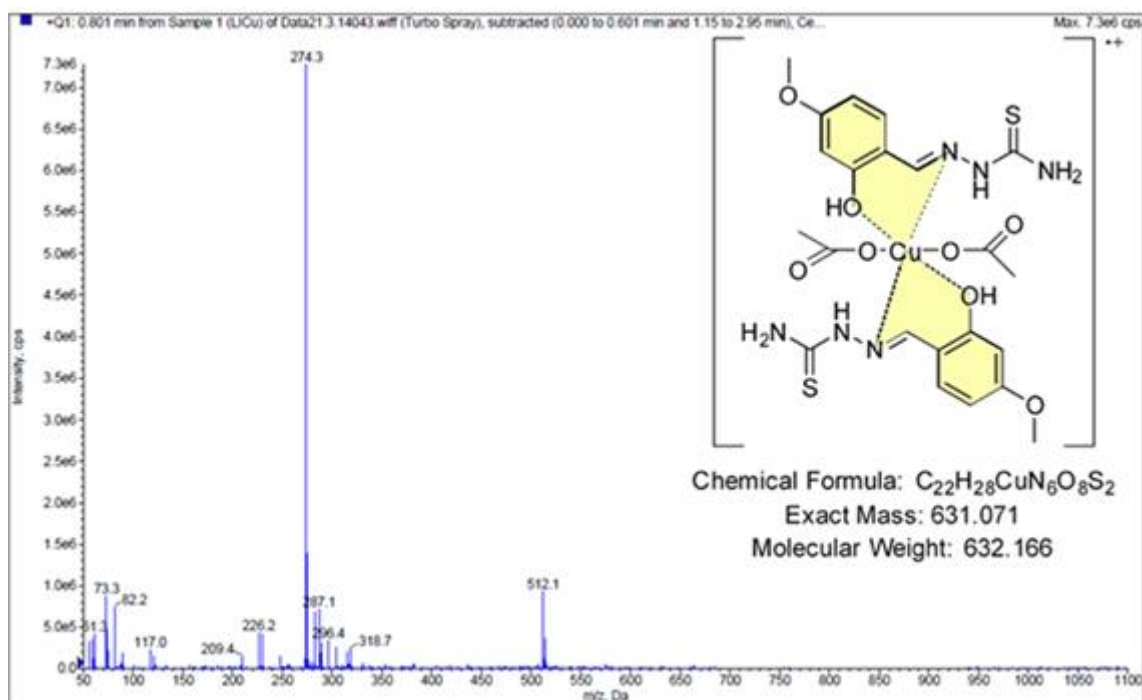


Fig (10) HNMR, <sup>13</sup>C spectrum of the ligand L1





**Fig. (14) Mas Spectrum of the complex [Co(L1) (H<sub>2</sub>O)<sub>2</sub>Cl<sub>2</sub>]**



**Fig. (15) Mas Spectrum of the complex [Cu(L1) (CH<sub>3</sub>COO)<sub>2</sub>]**

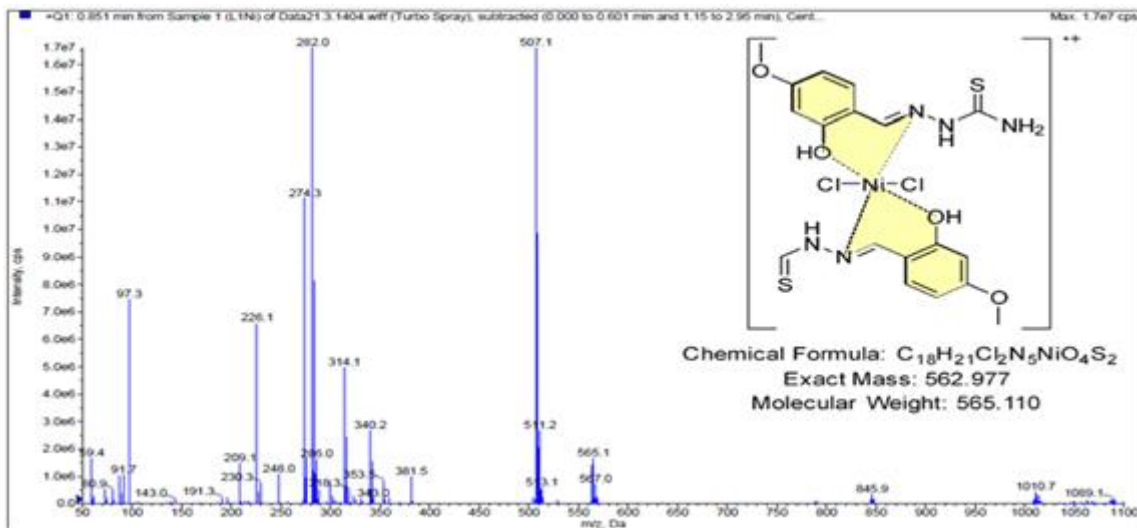


Fig. (16) Mass Spectrum of the complex [Ni(L1)Cl<sub>2</sub>]

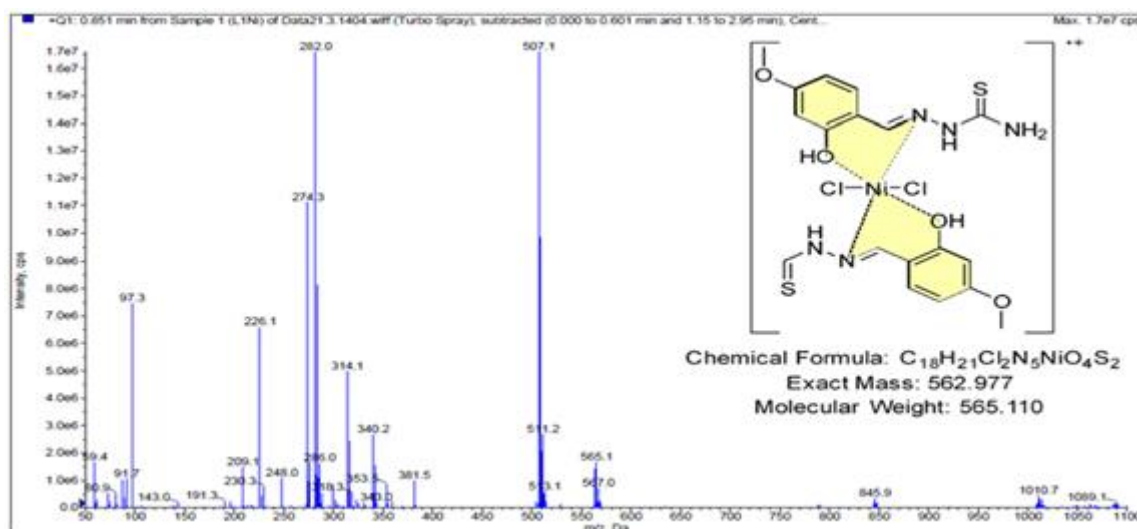


Fig. (17) Mass Spectrum of the complex [Ni(L2)]Cl<sub>2</sub>.2H<sub>2</sub>O

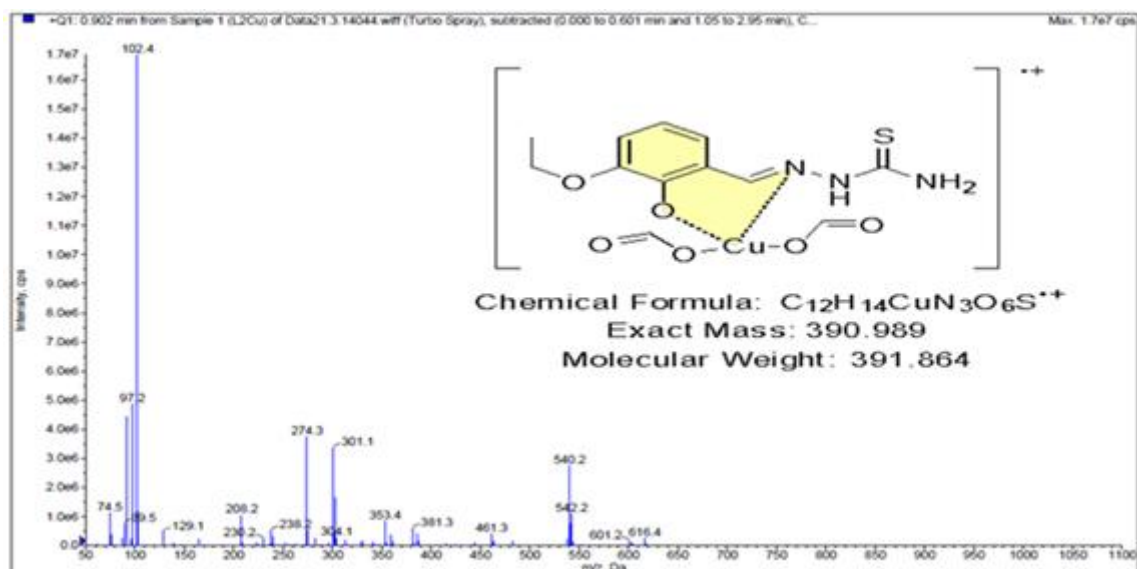
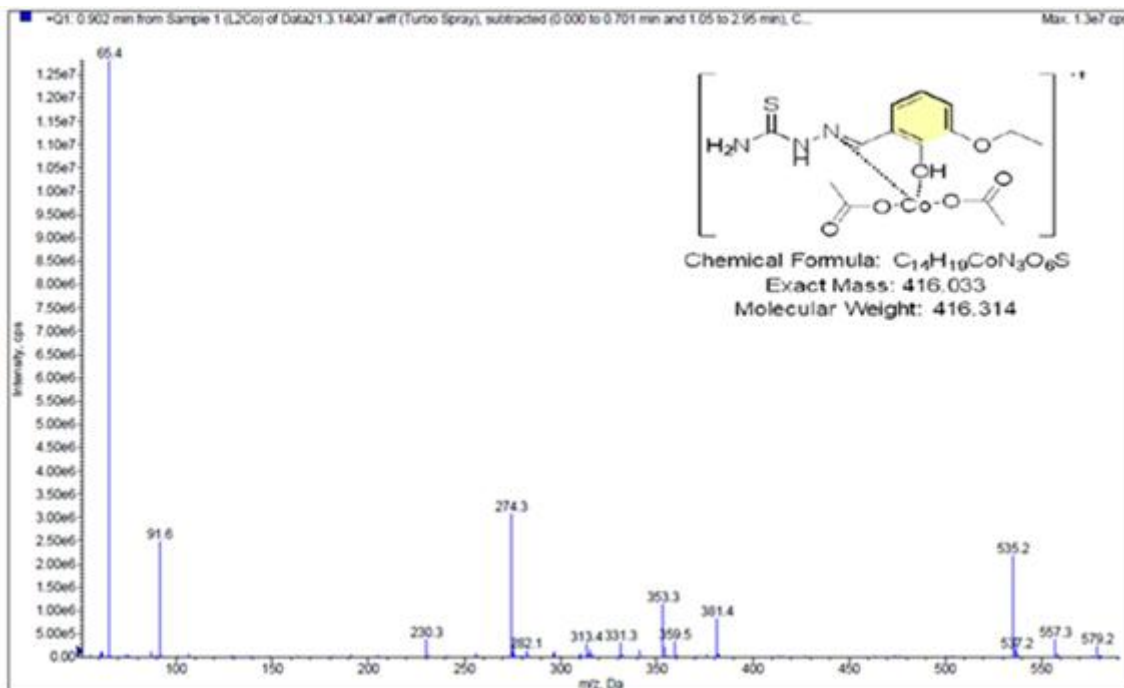


Fig. (18) Mass Spectrum of the Complex [CuL<sub>2</sub>(HCOO)<sub>2</sub>]



**Fig. (19) Mass Spectrum of the complex  $[CoL_2(CH_3COO)_2]$**